Measurement of drag torque, lift off speed and rotordynamic force coefficients in a shimmed BFB

Luis San Andrés[1], Joshua Norsworthy[1]*

[1]Mechanical Engineering Dept. Texas A&M University College Station, TX, USA
Lsanandres@tamu.edu, joshua.norsworthy@bakerhughes.com

Abstract. Oil free microturbomachinery relies on gas bearings, in particular bump type foil bearings (BFBs), to make nearly frictionless systems with improved efficiency, long life and extended maintenance intervals. Rotors supported on generation I BFBs often show large amplitude sub synchronous whirl motions that limit their application into high speed conditions. Mechanically preloading a BFB through shimming is a common practice that improves rotordynamic performance. This paper quantifies the effectiveness of shimming on the forced performance of a BFB (L=38.1mm, D =36.5mm) that comprises of a single top foil and bump foil strip. The dry-friction torque (T) during startup is proportional to the applied load and increases with shim thickness. The bearing lift-off shaft speed, establishing operation with a gas film, also increases with load. The friction factor $f=T/(RW)$ during dry friction operation at start up increases with shim thickness albeit decreasing with applied load. Once the bearing is airborne, the bearing –shimmed or not– shows approximately the same low friction factor, f~0.05 under a specific load $W/(LD)$ ~ 20 kPa. Dynamic loads spanning 200 Hz to 450 Hz excite the BFB in a rotordynamics rig operating at 50 krpm (833 Hz). A static vertical load, $W/(LD)$ acts on the bearing. The bearing direct stiffnesses increase with increasing excitation frequency while the damping coefficients decrease slightly. The stiffnesses for the various BFB configurations offer unremarkable differences. The direct damping coefficients of the shimmed BFB are up to 30% larger than the coefficients of the original bearing. The frequency averaged material loss factor for BFB with 50 μm shims ($\bar{\gamma}$~0.62) is 25% larger than that for the original bearing ($\bar{\gamma}$~0.47). As expected, a shimmed BFB dissipates more mechanical energy than a BFB without shims.

Keywords: Gas foil bearings (GFB), Bump-type foil bearings

1   Introduction

Gas foil bearings (GFBs), bump type foil bearings in particular, provide reliable, low friction support to high-speed micro turbomachinery (<400 kW) [1]. Figure 1 presents a schematic view of a typical bump type foil bearing (BFB) comprised of one or more bump foil strip layers, a top foil, and a bearing cartridge. At high speed operation,

---

rotor-BFB systems often show large amplitude sub harmonic whirl motions resembling a rotordynamic instability. Refs. [2-4] show examples of such phenomena.

Refs. [5-7] demonstrate that adding a mechanical preload, by placing metal shim strips axially under the bump foil strip (under spring) or manufacturing the bearing ID with geometrical offsets, effectively increases the onset speed and magnitude of the undesirable sub synchronous whirl motions. Figure 1 also depicts a shimmed BFB.

The *shimming* engineering practice is simple and low cost. Schiffmann and Spakovsky [8], in a numerical study for shimmed BFBs, report that decreasing the bearing under spring compliance (increasing its stiffness) and increasing the static load can improve system stability (critical mass) and increase the onset speed of instability while the structural damping has only a marginal effect.

There is limited experimental data on the force coefficients and the startup and shut down performance of shimmed BFBs. To this end, dynamic load experiments are conducted on a BFB, with and without shims, to determine its rotordynamic force coefficients and material loss factor, a measure of its ability to dissipate mechanical energy from vibrations. Also measurements during transient rotor speed events evidence the lift off rotor speed as well as the drag torque for operation under contact (dry sliding) and airborne operation with a gas film.

2   Test Bump Foil Bearing

Figure 1 shows depictions of a typical BFB and another bearing with shims inserted at three circumferential locations (120º apart). Table 1 shows the nominal dimensions and specifications of the test bearing and metal shims used. Fig. 1 also includes a photograph of the test BFB with a metal shim inserted between the bearing cartridge (inner diameter) and the bump foil strip.
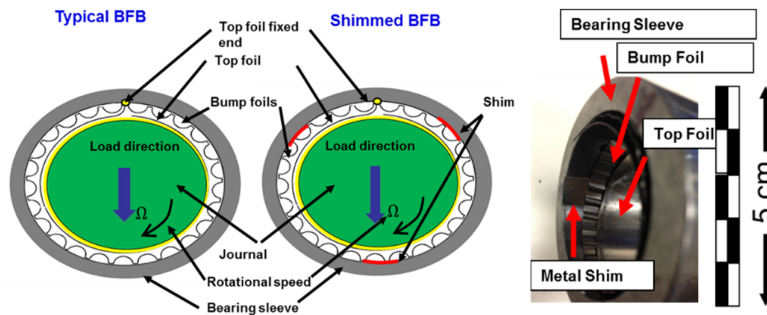
Fig. 1 Schematic representation of a typical first generation BFB and a shimmed BFB, and a photograph of a BFB with a metal shim layered axially through the bearing.

The commercially available shims feature a glue layer on one side, allowing their easy affixing to the bearing cartridge. The clearance in a bearing with shims [5] is periodic resembling that in a tri-lobe or three pad bearing. For a bearing with both 30 μm

shims and 50 μm shims, the clearance at the shim locations drops by 20% and 40%, respectively.

Table. 1 Nominal dimensions of test foil bearing and metal shims.

Parameters	Magnitude
Bearing cartridge outer diameter, D_O	50.74 mm
inner diameter, D_I	37.98 mm
Bearing axial length, L	38.10 mm
Rotor diameter, D_s (includes coating thickness)	36.5 mm
Top foil (Inconel X750), thickness t_T	0.12 mm
Foil length , $2\pi D_I$	110 mm
Number of bumps, N_B	26
Bump foil (Inconel X750), thickness, t_B	0.112 mm
Pitch, s_0	4.5 mm
Length, l_B	2.5 mm
Height, h_B	0.50 mm
Shims (AISI 4140) located 120º apart	
Length	38.1 mm
Thickness, t_s	0.050, 0.030 mm
Width	7.87 mm
Angular extent	11.8°
Measured inner diameter of the foil bearing (assembled)[2], D_A	36.74 mm
Nominal FB radial clearance[3], c_{nom}	0.120 mm

3   BFB friction factor: from dry-friction sliding to airborne operation

The current work keeps the same experimental procedure and test rig in Refs. [9,10]. Consult these references for details on the test rig, instrumentation, and measurement procedures used to record the drag torque of a test BFB. The bearing friction factor (*f*) is derived from the drag torque (*T*) and the applied external load (*W*), $f=T/(RW)$, with $R=\frac{1}{2} D_s$ as the rotor radius.

Figure 2 shows the friction factor (*f*) versus shaft speed for the test bearing, without and with shims, and operating under various specific loads, $W/(LD)\sim$6-20 kPa. Note the logarithmic scale on the vertical axes in the graphs of Figure 2. From start-up, at low shaft speeds, the rotor slides (rub or dry friction condition) on the top foil and the friction factor is large ($f\geq0.5$). The increase in friction between 0 krpm and 10 krpm is due to the shaft accelerating while still rubbing against the bearing. The drag torque and

---

[2] Measured via calipers with an uncertainty of ±0.005 mm
[3] Determined from the bearing dimensions as $c_{nom}=\frac{1}{2}(D_A-D_s)$, where D_A is the measured inner diameter of the bearing once assembled.

derived friction factor to overcome static friction, shown later in Figures 3 and 4, are obtained when the shaft first turns (0 krpm).

Above ~ 10 krpm the friction factor decreases rapidly until the rotor becomes airborne, i.e., with a gas film supporting the rotor. At $W/(LD)$~12 kPa, the airborne friction factor (f) of the bearing with 30 μm shims is similar to that of the original bearing, while the bearing with 50 μm shims has f ~15% higher than that of the bearing without shims. Once the rotor lifts, the friction factor changes little with rotor speed. At a shaft speed of 50 krpm (surface speed of 96 m/s), f decreases dramatically from 0.12 to 0.05 as the specific load increases from ~6 kPa to 20 kPa. The uncertainty in the friction factor is ±0.008.

## 4   Measurements during rotor acceleration tests. BFB friction factor at start-up and bearing lift off speed

The following results are derived from scrutiny of the measurements shown in Figure 2. The start-up or *breakaway* torque (T) depicted in Figure 3 is determined at 0 krpm, immediately prior to the shaft turning, and evidences eminently operation with dry friction or rubbing between surfaces (top foil and rotor). Note that T increases linearly with the applied load $W/(LD)$, as expected. T also increases, by up 40%, for the bearing with the thickest shims. The shims reduce the bearing clearance, bringing more surface area into contact with the rotor, thereby increasing the drag torque.

The rotor lift off speed establishes the transition from operation with the surfaces sliding to full film operation. Three rotor start-up and shut down tests were conducted for each BFB configuration, the maximum variability in lift off speed is ±2.5 krpm. The lift-off speed increases linearly with applied load, max. $W/(LD)$~ 20 kPa, and changes little whether the bearing has shims or not. Hence, no definite conclusion can be asserted as per one bearing configuration, with or without shims, permitting an early lift off condition.

Derived from the results in Fig. 3, Figure 4 shows that the bearing without shims has the lowest start-up (breakaway) dry friction factor, f ~ 0.31, nearly invariant with applied load to 20 kPa. The bearing with shims has a much larger f, albeit decreasing with load. The bearing with 50 μm shims has twice the friction factor of the original bearing at $W/(LD)$~6 kPa. However, at the highest load, $W/(LD)$~20 kPa, the bearing with 50 μm shims shows a 40% larger friction coefficient (f) than that of the original bearing.
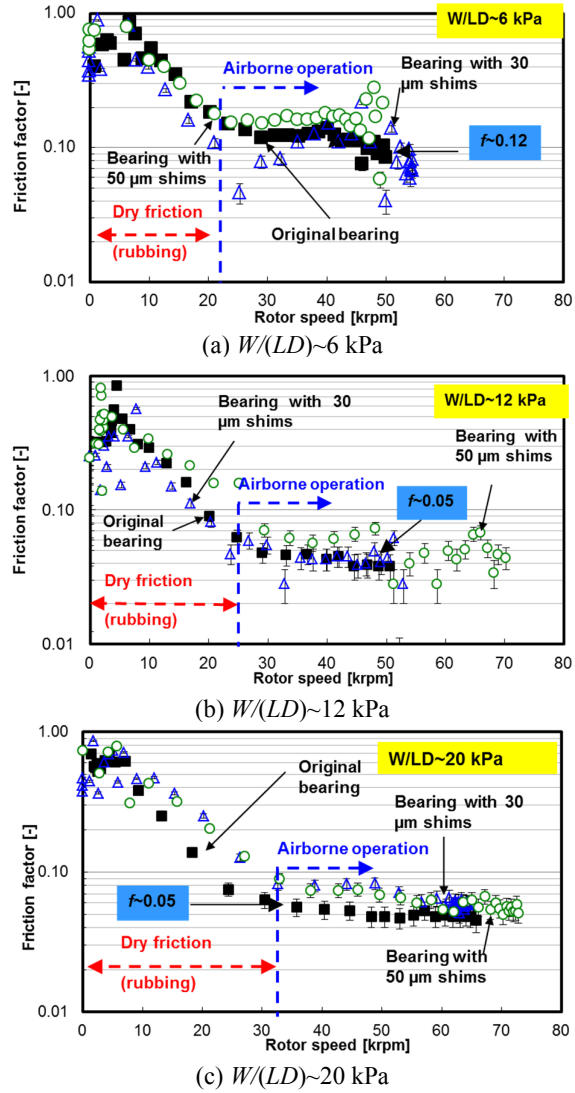
Fig. 2 Friction factor $f=T/(RW)$ versus rotor speed for the original BFB and bearing with shims of thickness 30 µm and 50 µm. Operation at specific load $W/(LD)$ (a) 6 kPa, (b) 12 kPa, (c) 20 kPa.
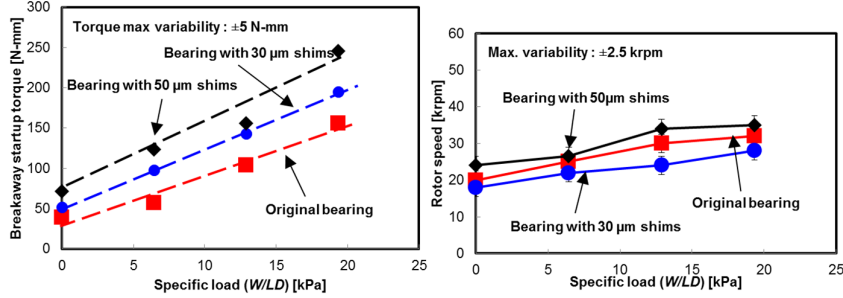
**Fig. 3** Breakaway torque and rotor lift off speed versus specific load, $W/(LD)$, for original BFB and BFB with shims of thickness 30 µm and 50 µm..
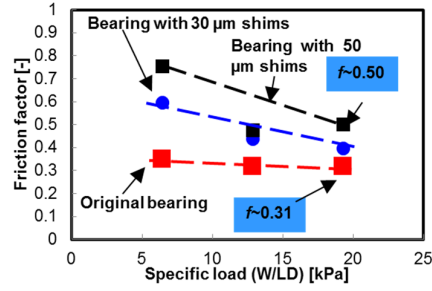
Fig. 4 Breakaway friction factor, $f=T/(RW)$, for dry-sliding operation versus specific load $W/(LD)$ for original BFB and bearing with shims of thickness 30 µm and 50 µm.

## 5 Rotordynamic force coefficients of a shimmed BFB

Refs. [10-12] describe a rotordynamic test rig to dynamically load a test BFB operating at a constant shaft speed and with an applied static vertical load (W). A frequency domain parameter identification process identifies the bearing force coefficients (stiffness and damping) from sine sweep dynamic loads applied to the test bearing along two orthogonal directions (45° from the vertical plane). The bearing displacement amplitude is kept at ~20 µm for all excitation frequencies.

Figure 5 shows the BFB stiffness coefficients $(K_{\alpha\beta})_{\alpha\beta=X,Y}$ versus excitation frequency (ω) for operation at 50 krpm (833 Hz) and with a static (vertical) load $W/(LD)$~14.3 kPa. The direct stiffnesses (K_{XX}, K_{YY}) of the bearing, without and with shims, increase with frequency. The cross coupled stiffnesses (K_{XY}, K_{YX}) are smaller than the direct ones, showing unremarkable change due to the addition of the shims. More importantly, the magnitude of the direct stiffnesses (K_{XX}, K_{YY}) is largely unchanged for the shimmed BFBs, i.e., the stiffnesses the original BFB are comparable to

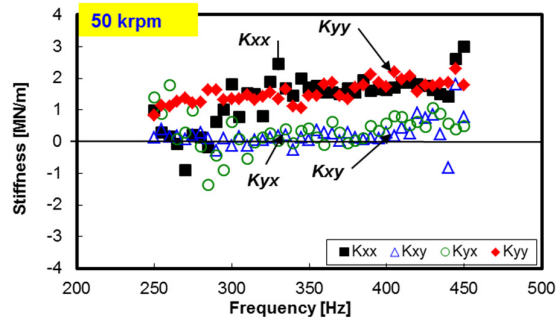those of the BFB with 30 μm shims and 50 μm shims. The uncertainty and variability in the stiffnesses are ±0.08 MN/m and ±0.1 MN/m, respectively; total= ±0.18 MN/m.
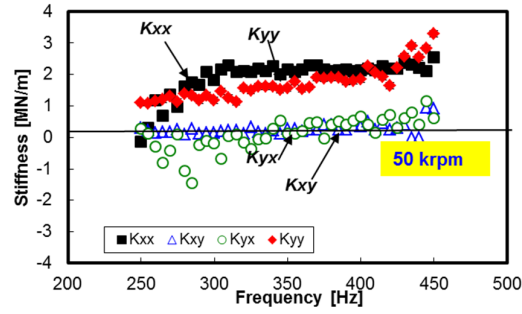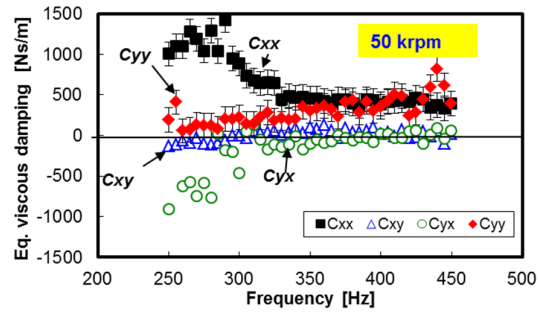

(a) Original bearing
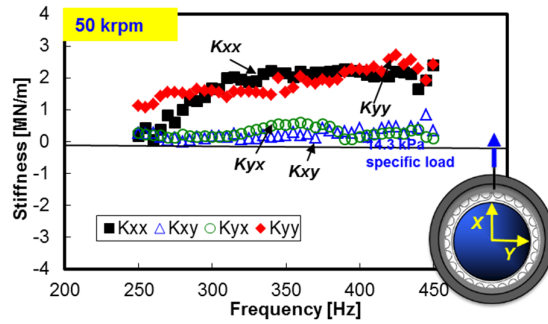
(b) Bearing with 30 um shims
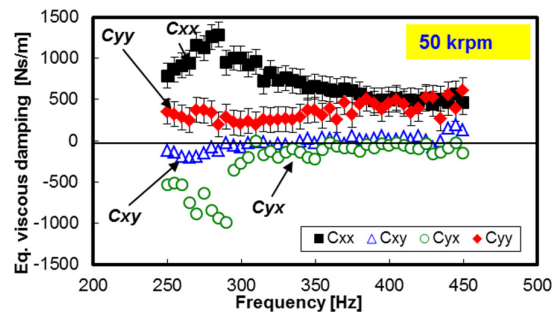

(c) Bearing with 50 um shims

Fig. 5 Stiffness coefficients versus excitation frequency for (a) original BFB, and bearing with (b) 30 μm shims and (c) 50 μm shims. Specific load $W/(LD)$~14.3kPa and shaft speed~50 krpm (833 Hz).

Figure 6 depicts the viscous damping coefficients $(C_{\alpha\beta})_{\alpha\beta=X,Y}$ for the original bearing and the bearing with shims. For frequencies 375 Hz to 450 Hz, C_{XX} and C_{YY} of the bearing with shims are larger than the coefficients of the original bearing; the increase is up to 30% for the bearing with 50 µm shims. Cross coupled coefficients are smaller than the direct ones and increase in magnitude for the bearing with shims.

(a) Original bearing

(b) Bearing with 30 um shims
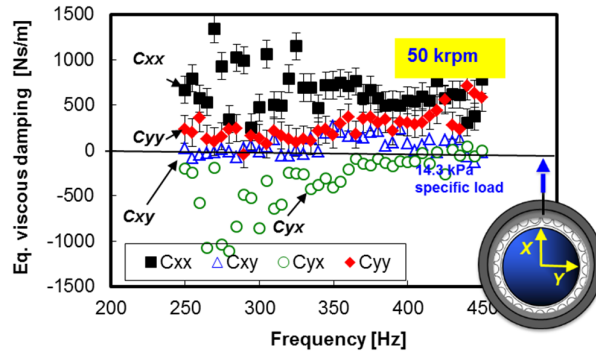
(c) Bearing with 50 um shims

Fig. 6 Damping coefficients versus excitation frequency for (a) original BFB, and bearing with (b) 30 µm shims and (c) 50 µm shims. Specific load $W/(LD)$~14.3kPa and shaft speed~50 krpm (833 Hz.

For the three bearing configurations, below 375 Hz, $C_{XX} > C_{YY}$ likely due to the static load applied in the vertical upward direction (X). C_{XX} later decreases with excitation frequency. From 375 Hz to 450 Hz the direct coefficients (C_{XX}, C_{YY}) are nearly equal. Note also $(C_{\alpha\beta})_{\alpha\beta=X,Y}$ for the BFB with 50 µm shims show a large scatter over the whole frequency range. The uncertainty and variability in damping coefficients is ±80 Ns/m and ±150 Ns/m, respectively; total = ±230 Ns/m.

The mechanical energy dissipation capability of a BFB is a combination of Coulomb dry friction and material hysteresis and is best quantified by a material loss factor (γ) [9]. The estimation of γ follows a development in Refs. [9, 10]; in brief $\gamma \sim K/(C\omega)$. San Andrés and Chirathadam [9] report a loss factor $\gamma \sim 0.5$ for a similarly sized BFB without shims.

Presently, for operation at a journal speed of 50 krpm (833 Hz), Figure 7 presents the loss factor (γ) versus excitation frequency (ω). γ varies little with frequency above 300 Hz, its maximum variability is ±0.05. At frequencies below 300 Hz, the large loss factor ($\gamma > 1$) is due to the small direct stiffness and large magnitude damping coefficients (see Figures 5 and 6) arising from a low displacement amplitude near the lowest excitation frequency. Note that the scatter in γ for the bearing with 50 µm shims is due to the scatter of the bearing direct force coefficients (see Figures 5 and 6).
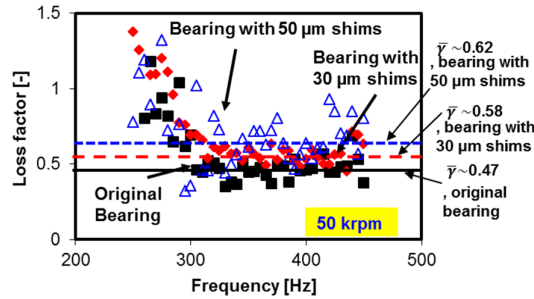
Fig. 7 BFB material loss factor (γ) versus excitation frequency for the original bearing (without shims) and a bearing with shims of thickness 30 µm and 50 µm. Specific load $W/(LD) \sim 14.3$kPa and shaft speed~50 krpm (833 Hz).

Let ($\bar{\gamma}$) be an average loss factor over a fraction of the test frequency range, from 300- 400 Hz [12]. $\bar{\gamma} = 0.47$ for the original bearing with a standard deviation $\sigma = 0.07$. The bearing with 50 µm shims shows $\bar{\gamma} \sim 0.62$ ($\sigma = 0.15$), a 25% increase. The bearing with shims apparently dissipates more mechanical energy. This assertion is obscured by the large standard deviation, however.

In a simple mechanical system operating with dry friction, $\gamma \sim f$ in theory [13]. The increase in $\bar{\gamma}$ for the shimmed BFB is likely due to an increase in the relative motion of the bump foils' crests and valleys against the top foil and bearing cartridge.

9

6   Conclusion

This paper presents measurements characterizing the static and dynamic performance of a BFB with three shims of two thicknesses (30 µm and 50 µm). For operation with dry friction, at the onset of shaft motion, the bearing with the thickest shims (50 µm) shows twice as large friction factor as the original bearing for the lowest load (5 kPa) albeit decreasing as the load increases. Once airborne, the BFB, with or without shims, operates with a low friction factor, $f\sim0.05$ at $W/(LD) \sim12$ kPa, that decreases with increasing applied load.

The bearing force coefficients are estimated over a frequency range of 200-450 Hz and under a specific static load, $W/(LD) \sim14.3$ kPa. The bearing dynamic displacements are kept at 20 µm, a fraction of the bearing cold clearance (120 µm). The shims have little effect on the bearing direct stiffness coefficients; however they appear to increase the direct damping coefficients, in particular along the static load direction.

The BFB (frequency averaged) material loss factor $\bar{\gamma}\sim0.47$ for the original BFB without shims and $\bar{\gamma}\sim0.62$ for the bearing with 50 µm shims. Note, however, that the standard deviation for $\bar{\gamma}$ in the bearing with 50 µm shims ($\sigma=0.15$) is twice as large as that of the original bearing ($\sigma=0.07$). See Ref. [12] for validation of the rotordynamic performance of a rotor supported on a BFB, without and with shims. Hence, as expected, a shimmed BFB dissipates a little more mechanical energy than the original bearing (without shims).

7   Acknowledgements

References

1. DellaCorte, C., 2011, "Stiffness and Damping Coefficient Estimation of Compliant Sur-face Gas Bearings for Oil-Free Turbomachinery," STLE Tribol. Trans., **54** (4), pp. 674-684.
2. Kim, T.H., and San Andrés, L., 2008, "Heavily Loaded Gas Foil Bearings: A Model Anchored to Test Data," ASME J. Eng. Gas Turbines Power, **130**, p. 012504.
3. Kim, T.H., and San Andrés, L. 2008, "Forced Nonlinear Response of Gas Foil Bearing Supported Rotors", Tribol. Int., **41**, pp. 704-715.
4. Kim, T.H., Rubio, D., and San Andrés, L., 2007, "Rotordynamic Performance of a Rotor Supported on Bump Type Foil Gas Bearings: Experiments and Predictions," ASME J. Eng. Gas Turbines Power, **129**, pp. 850-857.
5. Kim, T. H., and San Andrés, L., 2009, "Effects of a   Mechanical Preload on the Dynamic Force Response of Gas Foil Bearings - Measurements and Model Predictions," STLE Tribol. Trans., **52**, pp. 569-580.
6. Sim, K., Lee, Y-B., Kim, T.H., and Jangwon L., 2012, "Rotordynamic Performance of Shimmed Gas Foil Bearings for Oil-Free Turbochargers", ASME J. Tribol., **134**, p. 031102.

7. Sim, K., Koo, B., Lee, J.S., and Kim, T.H., 2014,"Effects of Mechanical Preload on the Rotordynamic Performance of a Rotor Supported on 3 Pad Gas Foil Bearings", ASME Paper No. GT2014-25849.

8. Schiffmann, F., and Spakovszky, Z.S., 2013, "Foil Bearing Design Guidelines for Improved Stability," ASME J.Tribol., **135**, p. 011103.

9. Chirathadam, T. A., and San Andrés, L., 2012, "A Metal Mesh Foil Bearing and a Bump-Type Foil Bearing: Comparison of Performance for Two Similar Size Gas Bearings," ASME J. Eng. Gas Turbines Power, **134**, p. 102501.

10. Chirathadam, T.A., 2012, "Metal Mesh Foil Bearings: Prediction and Measurement of Static and Dynamic Performance Characteristics," Ph.D Thesis, Texas A&M University, College Station, TX.

11. Chirathadam, T. A., Kim, T.H, Ryu, K., and San Andrés, L., 2010, "Measurements of Drag Torque, Lift-Off Journal Speed and Temperature in a Metal Mesh Foil Bearing," ASME J. Eng. Gas Turbines Power, **132**, p. 112503.

12. Norsworthy, J.D., 2014, "Measurement of Drag Torque, Lift Off Speed, and Identification of Frequency Dependent Stiffness and Damping Coefficients of a Shimmed Bump-Type Foil Bearing," M.S. Thesis, Texas A&M University, College Station, TX.

13. Ginsberg, J., 2001, Mechanical and Structural Vibrations-Theory and Applications, Wiley, New York, pp. 137-138.